PRIMARY RESEARCH ARTICLE

Global Change Biology WILEY

The greening of the Northern Great Plains and its biogeochemical precursors

E. N. Jack Brookshire[1] 📧 | Paul C. Stoy[1,2] | Bryce Currey[1] | Bruce Finney[3]

[1]Department of Land Resources and Environmental Sciences, Montana State University, Bozeman, MT, USA

[2]Department of Biological Systems Engineering, University of Wisconsin–Madison, Madison, WI, USA

[3]Departments of Biological Sciences and Geosciences, Idaho State University, Pocatello, ID, USA

Correspondence
E. N. Jack Brookshire, Department of Land Resources and Environmental Sciences, Montana State University, Bozeman, MT, USA.
Email: jbrookshire@montana.edu

Abstract

Vegetation greenness has increased across much of the global land surface over recent decades. This trend is projected to continue—particularly in northern latitudes—but future greening may be constrained by nutrient availability needed for plant carbon (C) assimilation in response to CO_2 enrichment (eCO_2). eCO_2 impacts foliar chemistry and function, yet the relative strengths of these effects versus climate in driving patterns of vegetative greening remain uncertain. Here we combine satellite measurements of greening with a 135 year record of plant C and nitrogen (N) concentrations and stable isotope ratios ($\delta^{13}C$ and $\delta^{15}N$) in the Northern Great Plains (NGP) of North America to examine N constraints on greening. We document significant greening over the past two decades with the highest proportional increases in net greening occurring in the dries and warmest areas. In contrast to the climate dependency of greening, we find spatially uniform increases in leaf-level intercellular CO_2 and intrinsic water use efficiency that track rising atmospheric CO_2. Despite large spatial variation in greening, we find sustained and climate-independent declines in foliar N over the last century. Parallel declines in foliar $\delta^{15}N$ and increases in C:N ratios point to diminished N availability as the likely cause. The simultaneous increase in greening and decline in foliar N across our study area points to increased N use efficiency (NUE) over the last two decades. However, our results suggest that plant NUE responses are likely insufficient to sustain observed greening trends in NGP grasslands in the future.

KEYWORDS
climate, grasslands, isotopes, nitrogen cycle, nitrogen use efficiency, Northern Great Plains, vegetative greening, water use efficiency

1 | INTRODUCTION

Field experiments and ecosystem models suggest that recent vegetative greening is largely explained by CO_2 enrichment (eCO_2), climate change, N deposition, and land cover change (Huang et al., 2018; Zhu et al., 2016). While the relative importance of these drivers varies geographically (Huang et al., 2018; Mao et al., 2016; Myneni, Keeling, Tucker, Asrar, & Nemani, 1997; Zhu et al., 2016), eCO_2 is the most spatially uniform and its direct effects on plant physiology are well understood. Free-atmosphere CO_2 enrichment (FACE) studies show increased plant carbon (C) assimilation and photosynthetic nitrogen (N) use efficiency (NUE) with eCO_2 (Feng et al., 2015; Leakey et al., 2009; Terrer et al., 2018). These effects are strongest among C3 plants that dominate land–atmosphere C exchange globally (Still, Berry, Collatz, & DeFries, 2003). However, these studies also show that foliar N concentrations decline by ~6%–12% below that at ambient CO_2 due to diminished N acquisition (Feng et al., 2015), availability (Reich & Hobbie, 2013), or assimilation (Busch, Sage, & Farquhar, 2018).

Nitrogen is fundamental to C assimilation and protein synthesis in leaves and thus could constrain greening, particularly in N-limited ecosystems. Herbarium and tree-ring analyses indicate that declines in plant N have already occurred across some temperate biomes over the last century despite increases in N deposition (Craine et al., 2018; McLauchlan, Ferguson, Wilson, Ocheltree, & Craine, 2010; McLauchlan et al., 2017; Peñuelas & Estiarte, 1996; Peñuelas & Matamala, 1990), consistent with the hypothesis that N is constraining greening (Hungate, Dukes, Shaw, Luo, & Field, 2003; Luo et al., 2004; McMurtrie et al., 2008). Simultaneously, these studies document large and persistent increases in plant intrinsic water use efficiency (iWUE) in response to eCO_2 (Frank et al., 2015; McLauchlan et al., 2010), a response that reduces water costs per unit C assimilated and thus could potentially sustain vegetative greening, particularly in drier regions (Zhu et al., 2016).

It is unclear whether increased iWUE and/or NUE can compensate for increasing N demand under scenarios of enhanced vegetative productivity. Insight into these processes can be gained by understanding how leaf-level intercellular CO_2 (C_i), the core substrate for photosynthesis, has changed relative to atmospheric CO_2 (C_a) over time. Nitrogen and C_i are fundamentally coupled through the action of the Rubisco enzyme, which typically accounts for ~25% of leaf N (Leakey et al., 2009). If C_i/C_a ratios remain roughly constant, eCO_2 would drive increases in C_i and photosynthetic C assimilation. Given the strong dependence of C assimilation on C_i, alternative explanations that result in constant C_i imply large reductions in stomatal conductance (Guerrieri et al., 2019) and potentially constant leaf N/C_i ratios depending on physiological responses to increasing C_a. Under N-limited conditions, however, FACE results document Rubisco acclimation, declines in Rubisco content, accumulation of foliar carbohydrates (Leakey et al., 2009),

and declines in photorespiratory N assimilation (Busch et al., 2018) under eCO_2. Knowledge of C_i change is crucial for understanding changes in plant NUE and C:N stoichiometry, which can drive ecosystem-level N availability via effects on microbial N immobilization and mineralization (Luo et al., 2004). However, the role of these key interactions in shaping recent and future vegetation changes remain poorly understood.

Temporal changes in the $\delta^{15}N$ composition of leaves offers one way to diagnose long-term change in the plant–soil N cycle. While several processes can imprint on $\delta^{15}N$ in foliage including external N inputs, mycorrhizal discrimination, and enzymatic discrimination during nitrate assimilation, numerous lines of evidence also indicate that the leaf $\delta^{15}N$ signature tracks changes in inorganic N availability (Craine et al., 2009), consistent with increasing microbial fractionation in soils as inorganic N availability increases (Craine et al., 2015). Declines in foliar $\delta^{15}N$ in response to experimental eCO_2 have been documented across numerous plant types and ecosystems (BassiriRad et al., 2003) and long-term declines in $\delta^{15}N$ from herbarium and tree-ring studies have been documented over the last century across many ecosystems globally (Craine et al., 2018; McLauchlan et al., 2010, 2017; Peñuelas & Estiarte, 1996), suggesting direct or indirect effects of eCO_2 on N availability. Yet, it is unclear how the recent increases in vegetative productivity, which in the northern hemisphere have been evident since at least the 1960s (Keeling, Chin, & Whorf, 1996), relate to changes in plant N and $\delta^{15}N$ in N-limited ecosystems and if these relationships vary across climatic gradients.

The extent to which changes in foliar chemistry and vegetative activity are coupled in space and time may provide insight into the relative strength of global change drivers. For example, while the rise in C_a has directly increased plant iWUE through enhanced
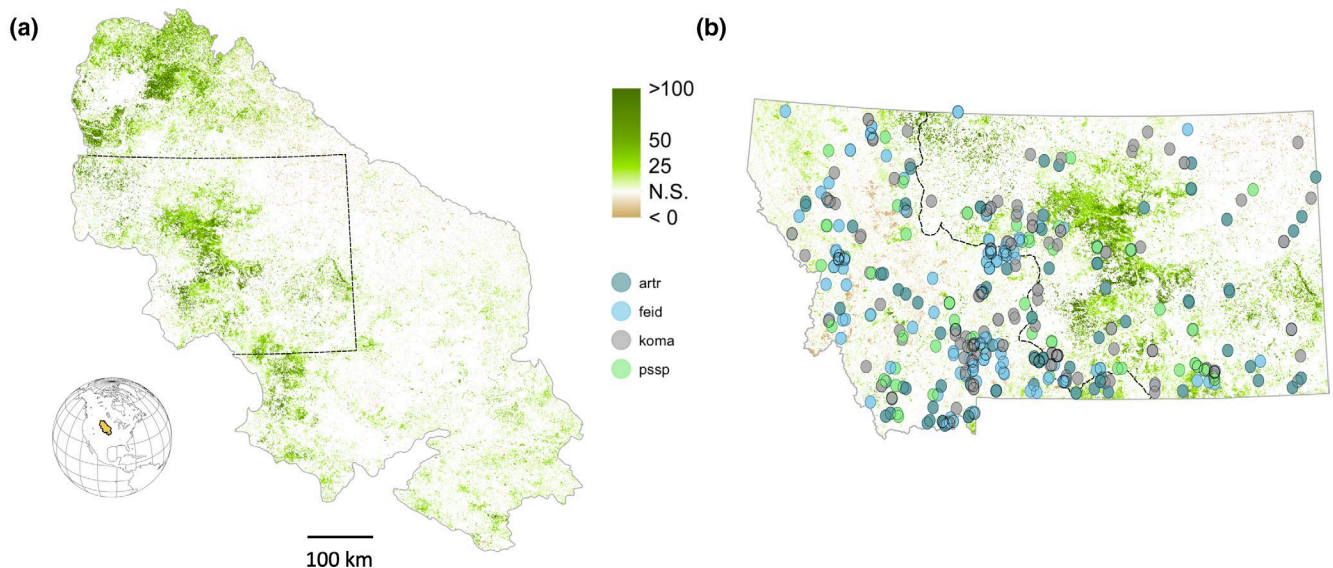
FIGURE 1 Recent patterns of vegetation greening across the Northern Great Plains (NGP) of North America. Percent change in NDVI from 2000 to 2018 across the NGP (a). White areas show pixels with no evidence of significant change. The inset in (a) shows study area location within the NGP (tan color). Distribution of herbarium samples across the NGP and Northern Rocky Mountains (NRM) of MT (b). Species are *Artemisia tridentata* (artr), *Festuca idahoensis* (feid). *Koeleria macrantha* (koma) and *Pseudoregeneria spicata* (pssp). The dashed line indicates the boundary between the NGP (east) and NRM (west) ecoregions. NDVI, normalized difference vegetation index

photosynthesis in addition to reduced transpiration through stomata (Guerrieri et al., 2019), much of the recent increase in northern hemisphere vegetative greening is thought to be driven by changes in climate and increased growing season length. For N, the degree to which changes in plant N may also be coupled directly or indirectly to eCO_2 and greening is less clear.

Here we combine satellite observations of recent vegetation greening trends with chemical and isotopic analyses of historical plant samples to examine responses of vegetative productivity to eCO_2 and climate in the Northern Great Plains (NGP) of North America. The NGP is one of the largest relatively intact temperate grasslands worldwide (Auch, Sayler, Napton, Taylor, & Brooks, 2011), is strongly N-limited (Burke, Lauenroth, & Parton, 1997), has experienced a strong wetting trend over the last 20 years (Bromley, Gerken, Prein, & Stoy, 2020; Rodell et al., 2018), and is projected to experience increases in growing season precipitation (Stoy et al., 2018) and vegetation greening (Hufkens et al., 2016; Reeves, Moreno, Bagne, & Running, 2014; Shafer, Bartlein, Gray, & Pelltier, 2015) over the next century. To examine the spatial and temporal correspondence of any potential changes in foliar chemistry and vegetative greening, we analyzed monthly Moderate Resolution Imaging Spectroradiometer (MODIS) normalized difference vegetation index (NDVI) data as a proxy for photosynthetically active vegetation across the NGP for the 2000–2018 period and leaf C and N concentrations and stable isotopes of common C_3 plants collected from 1881 to 2016 across 390 grassland sites spanning broad environmental gradients across the NGP and Northern Rocky Mountain (NRM) ecoregions (Table S1) in the US State of Montana (MT; Figure 1a,b). As mean climate is on average considerably cooler and wetter in the NRM compared to the NGP, we used this contrast to evaluate the climate sensitivity of any changes in vegetative activity and foliar iWUE, chemistry and $\delta^{15}N$ and their interactions.

2 | MATERIALS AND METHODS

2.1 | Satellite NDVI data

Normalized difference vegetation index data were derived from the NASA's MODIS Vegetation Indices 16 day L3 Global product (MOD13A1, version 6) at a 0.5 km spatial scale. Pixel-level NDVI is generated from daily surface-reflectance data aggregated every 8 days and composited every 16 days, from which the maximum value is selected at each pixel. An annual time series of bi-monthly NDVI values was used to calculate annual maximum NDVI. We used a two-sided Mann–Kendall trend test to determine which pixels showed significant ($p < .05$) positive or negative change over the 2000–2018 period. For pixels showing positive ("greening") or negative ("browning") NDVI change over time, we calculated percent change relative to the initial NDVI value. In total, we analyzed changes in NDVI across 1,037,074 pixels comprising the entire NGP and 616,199 pixels spanning the NGP and NRM of MT. For each region, we determined net greening rates by multiplying the fraction

of pixels showing significant positive, negative, or no NDVI change by their respective mean (±geometric *SD*) magnitude NDVI change (% per year).

2.2 | Climate and nitrogen deposition

We estimated mean annual temperature (MAT) and precipitation (MAP) across the NGP and NRM of MT using CHELSA (Climatologies at high resolution for the earth's land surface areas) data of downscaled model output temperature and precipitation at 1 km resolution for the 1980–2018 period (Karger et al., 2017). We also used PRISM (Parameter-elevation Regressions on Independent Slopes Model; http://prism.oregonstate.edu) to calculate the long-term (1890–2016) growing season (May–August) Palmer Drought Severity Index (higher values indicate wet conditions and lower values indicate drought) for major hydrologic units in the NGP (Fort Peck Reservoir, Big Horn, Powder River) and NRM (Marias, Missouri Headwaters, Upper Yellowstone) of MT in which most of our plant samples were collected and for the individual coordinates of our field collections. To examine long-term patterns of external N inputs, we used annual bulk NO_3-N + NH_4-N deposition measured from 1984 to 2017 by the National Atmospheric Deposition Program at five stations in MT (MT00, MT07, MT98, MT96, MT97).

2.3 | Herbarium data

We selected four native C3 grassland species (*Artemisia tridentata*, *Festuca idahoensis*, *Koeleria macrantha*, *Pseudoroegeneria spicata*; Table S1) for study based on (a) documented broad geographic distribution and high relative abundance across NGP and NRM grasslands (Lavin & Seibert, 2011; Mueggler & Stewart, 1980) and (b) broad spatial representation of herbarium type specimens in the Consortium of Pacific Northwest Herbaria (CNHP) database (http://www.pnwherbaria.org) for which Montana samples are housed at the Montana State University Herbarium. Though C_4 grass species occur within our study area, these species compose a small proportion of Montana grassland communities. The CNHP records the spatial coordinates, date of sampling and site descriptions documented by the original botanical collectors. We accessed all available specimens of our study species and sampled small sections of leaf material from 3 to 5 leaves per specimen based on availability. Subsamples of each specimen were gently cleaned with a brush and were composited and ground for chemical and isotopic analysis.

2.4 | Plant resampling

In 2016, we resampled plants from a randomly chosen subset ($n = 80$) of the original site locations (Table S1). We incorporated historical site descriptions to relocate the original sampling location given potential inaccuracies in the reported coordinates and altitude

and resampled within 3 weeks of the original collection date. Sites with significant disturbance or land-use change or that were not publicly accessible were excluded. After field collections, we cross-checked our recorded site altitudes with those of historical samples and excluded those that differed by >100 m to avoid potential effects of climate and atmospheric pressure on chemical and isotope distributions. Resultant samples (n = 68) were processed identically to the historical herbarium specimens.

2.5 | Chemical and isotopic analyses

Samples for carbon and nitrogen concentrations and stable isotope ratios were analyzed at the Idaho State University Stable Isotope Laboratory using a Costech ECS 4010 elemental analyzer interfaced with a Thermo Delta V Advantage continuous flow isotope ratio mass spectrometer. All stable isotopic data are reported in standard delta notation ($\delta^{13}C$, $\delta^{15}N$) relative to the Vienna PeeDee Belemnite and atmospheric N_2 reference standards. Analytical precision, calculated from analysis of standards distributed throughout each run, was ≤±0.2‰ for both C and N stable isotopes, and <±0.5% of the sample value for %N and %C. To account for the changing ^{13}C signature of C_a, we used the average $^{13}CO_2$ signature for June–September months spanning the 1978–2016 period recorded at La Jolla, CA and Point Barrow, AK, USA (Scripps Institution of Oceanography). To derive CO_2 and $^{13}CO_2$ signatures for the period 1881–1978, we used ice-core records (Francey et al., 1999) and interpolated missing data using a spline function. We calculated ^{13}C discrimination (Δ) as

$$\Delta = \frac{\delta^{13}C_{air} - \delta^{13}C_{plant}}{1 + \delta^{13}C_{plant}/1{,}000}, \tag{1}$$

which we used to derive C_i/C_a, C_i, and iWUE by applying isotope fractionation constants for carboxylation (b, 27‰) and diffusion (a, 4.4‰; Farquhar, Ehleringer, & Hubick, 1989).

$$\frac{C_i}{C_a} = \frac{\Delta - a}{b - a}, \tag{2}$$

$$C_i = \frac{C_a \Delta - C_a a}{b - a}, \tag{3}$$

$$\text{iWUE} = \frac{C_a \left(1 - \frac{C_i}{C_a}\right)}{1.6}. \tag{4}$$

2.6 | Statistical analyses

We analyzed changes in regional climate and foliar chemistry and isotopes over time using a combination of linear and non-linear regression and breakpoint analysis to detect changes in slope using packages "nlme" and "segmented" in R. For break-point analyses, we used Z-scores of foliar chemistry and isotope data to visualize long-term dynamics on a common scale. We examined the relative

strength of eCO_2 versus climate effects on foliar chemistry and $\delta^{15}N$ using linear mixed effects models either with C_a or C_i as fixed effects and species, year, or climate as random effects or with climate as a fixed effect and species and year as random effects. We retained species as a random effect in all models. To examine climate in these models we used the growing season PDSI which has been shown to predict climate sensitivity in MT grasslands (Brookshire & Weaver, 2015). Because PDSI did not change directionally over time while C_a did, we nested species within year to isolate climate effects from non-linear increases in C_a due to eCO_2. We chose models with the lowest corrected Akaike information criterion (AICc) using an AICc difference (ΔAICc) between models of >2 as a significance cut-off (Anderson, 2007). All models were best explained without climate effects. We developed species-specific C_i response curves using the general form

$$N_s = \frac{N_{min}C_i}{k_m + C_i}, \tag{5}$$

where N_s is the species-specific response variable (i.e., %C, %N, $\delta^{15}N$), N_{min} is the minimum (or maximum) value and k_m is the half-saturation constant. While linear regressions generally explained foliar responses to C_i equally well as saturating functions (ΔAICc < 2), we assumed that C and N concentrations have species-specific physiological minima and maxima and thus cannot increase or decrease indefinitely or fall below zero, as linear regressions imply. Finally, to simulate potential maximum changes in foliar chemistry in response to future eCO_2 we applied Representative Concentration Pathway 8.5 projected C_a for year 2100 to species-specific CO_2-C_i regressions and functional curves for %C, %N, and molar C:N ratios.

3 | RESULTS

3.1 | Recent trends in vegetative activity

We document extensive vegetative greening across the NGP biome over the last two decades. Sustained increases in NDVI were evident across >19% of the land area at an average rate of 1.2% per year, a 22% increase since 2000. By combining the distribution and rates of browning (declining NDVI) pixels, we calculate a net positive increase in peak vegetative activity greater than 0.2% per year across the NGP as a whole. Greening rates were especially pronounced across the MT portions of the NGP (Figure 1; Table 1). In contrast, net greening rates were fourfold lower in the mountainous and largely forested NRM part of our study area. This difference resulted from a higher proportion of the NRM that experienced browning and a greater than twofold lower magnitude of increase among greening pixels compared to the NGP.

Comparing long-term (1980–2018) mean climate across our MT study area with recent changes in NDVI revealed that greening trends were more prevalent in the driest and warmest areas and increased most strongly with increasing MAT (Figure 2a) and declining MAP (Figure 2b) in the NGP compared to the NRM. The spatial locations of our historical plant samples are well represented across

the geographic distribution of vegetative trends and climate space within our study area (Figure 2c).

3.2 | Long-term changes in foliar chemistry and isotope distributions

Despite large variation in mean annual climate (Figure 2a,b) and decadal variation in growing season climate across our study area (Figure 3a), C_i increased in all species regardless of geographic location (Figure 3c), while isotopic discrimination and C_i/C_a ratios remained constant (Figure S1). The increase in C_i accelerated sharply in the 1970s (break-point analysis mean and standard deviation: 1973 ± 4 years; $p < .001$; Figure 3c) and was strongly correlated with C_a but not changes in climate (Figure S1). Accordingly, we find that iWUE has increased on average by 37% over the last century, most of which (85%) has likewise occurred since the early 1970s (1971 ± 7 years; $p < .001$; Figure 3e). Although the magnitude of response

TABLE 1 Geometric mean and geometric standard deviation range (in parentheses) of greening (increasing NDVI) and browning (decreasing NDVI) across the Northern Great Plains (NGP), the Montana (MT) portions of the NGP (MT_{NGP}), and the Montana portions of the Northern Rocky Mountains (MT_{NRM})

	NGP	MT_{NGP}	MT_{NRM}
Land area greening (%)	19.4	19.1	15.2
Land area browning (%)	2.2	1.2	7.6
Greening pixel rate (% per year)	1.21 (0.44–3.31)	1.53 (0.63–3.68)	0.56 (0.19–1.63)
Browning pixel rate (% per year)	−0.34 (−0.09 to −1.15)	−0.53 (−0.15 to −1.91)	−0.37 (−0.13 to −1.09)
Net greening rate (% per year)	0.23 (0.09–0.71)	0.28 (0.13–0.75)	0.06 (0.04–0.37)

Abbreviation: NDVI, normalized difference vegetation index.

varied among species (27%–53%), it did not vary systematically across climate regions.
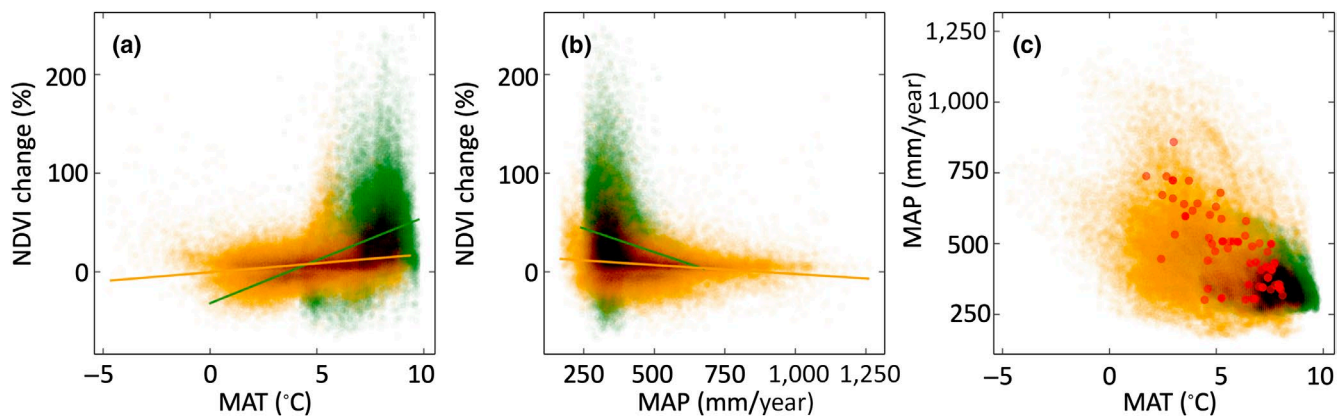
The timing and spatial uniformity of increases in C_i and iWUE suggest a direct effect of eCO_2 on leaf-level physiology regardless of climate. We next assessed whether leaf C and N concentrations have responded in an analogous manner or have changed in response to changing climate or atmospheric N deposition. Foliar C concentrations increased significantly over time (0.4 ± 4 mg g^{-1} year^{-1}, $p < .001$) but did not show a clear breakpoint nor vary as a function of PDSI. In contrast, foliar N concentrations declined significantly ($p < .01$) across all study species, but the decline began in the 1930s (1931 ± 13 years), roughly four decades prior to steep increases in C_a and iWUE and has not recovered since (Figure 3d). Foliar δ^{15}N also decreased by ~10% uniformly across the NGP and the NRM beginning in the late 1930s (1937 ± 13 years; $p < .01$; Figure 3f). While we found no long-term relationship between either foliar N and PDSI or δ^{15}N and PDSI ($p > .1$ in mixed effects models using species and year as random effects; Figure S2), we document that the onset of declining foliar N and δ^{15}N corresponded closely with the "Dust Bowl" drought of the 1930s (Figure 3a,d,f). In contrast to sustained declines in foliar N, measured N deposition rates have more than doubled (0.028 kg N ha^{-1} year^{-2}) since the 1980s (Figure 3b), but have remained relatively low (long-term deposition rate of 1.1 ± 0.6 kg N ha^{-1} year^{-1}) over the recent period of vegetative greening in the NGP.

We next asked if these findings, which rely on statistical fitting across samples collected at different years and locations, persist after controlling for geographic location. Analysis of our spatially paired samples confirms the magnitude and direction of change observed in the full data set. On average, foliar C concentrations increased by 10 ± 1% (4%–17% among species), N decreased by 12 ± 3% (6%–18%), C:N ratios increased by 19 ± 3% (13%–30%) and δ^{15}N decreased by 10 ± 2% (6%–18%) independent of wide variation in local growing season climate (Figures S3 and S4). Furthermore, there was no evidence ($p > .05$) within and across species that proportional declines in leaf N or δ^{15}N depend on

FIGURE 2 Distribution of vegetative greening rates across our study area. Shown is NDVI change over the 2000–2018 period in the NGP (green points and regression lines) and NRM (orange points and regression lines) as a function of mean annual temperature (MAT) (a) and precipitation (MAP; b). Panel (c) shows the distribution of 2016 herbarium sampling locations across climate space of the NGP and NRM. NDVI, normalized difference vegetation index; NGP, Northern Great Plains; NRM, Northern Rocky Mountains
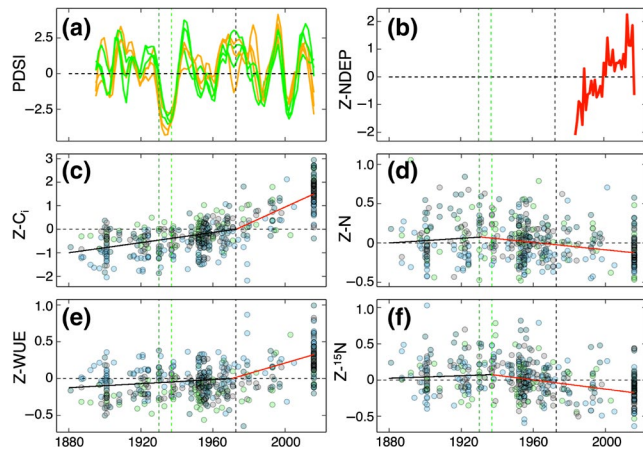
FIGURE 3 Regional climate patterns and vegetation chemical change. Time series of growing season Palmer Drought Severity Index (PDSI; lower values indicate drought conditions) for hydrologic basins in the NGP (green lines) and NRM (orange lines; a). Z-scores of atmospheric N deposition (NDEP) (b), leaf internal CO_2 (C_i) concentrations (c), foliar N (d), water use efficiency (WUE; e), and foliar $\delta^{15}N$ (f). Vertical dashed lines show significant ($p < .05$) breakpoints in slope determined using segmented regression for N and $\delta^{15}N$ (green) and C_i (black). AICc was lowest in linear mixed effects models with species identity only as a random effect. Species colors in (c–f) are the same as in Figure 1. AICc, corrected Akaike information criterion; NGP, Northern Great Plains; NRM, Northern Rocky Mountains
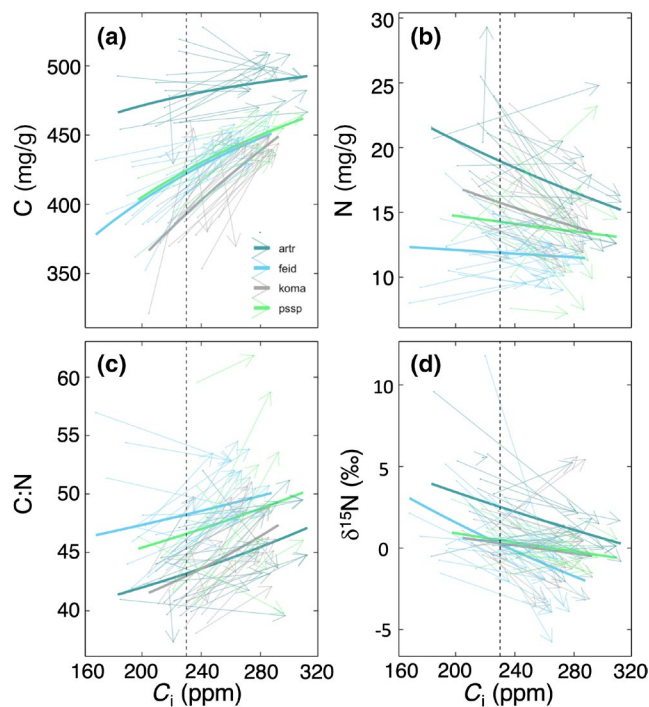
FIGURE 4 Functional response of foliar chemistry and $\delta^{15}N$ to increasing leaf internal CO_2 concentration (C_i). Species-specific saturating curves for foliar %C (a), %N (b), foliar C:N ratios (c), and $\delta^{15}N$ (d). Thin lines with arrows connect historic and contemporary samples and thick lines are fitted curves through all samples. Vertical dashed lines show the break-point year value of C_i

increases in C, as would be expected if declines were driven by foliar mass dilution.

Finally, we examined how foliar chemistry and $\delta^{15}N$ may have changed in response to non-linear increases in leaf C_i. We focused our analysis on the reduced (spatially paired) data set to control for local differences in climate and soil resource availability. Foliar C and C:N increased and N and $\delta^{15}N$ decreased significantly ($p < .01$) in response to the >100 ppm increase in C_i over the last century (Figure 4a–d). Furthermore, across broad geographic areas and climate zones, our four study species converged toward an increasingly similar and narrow range of foliar chemistry with increasing C_i. Relatively C-rich species tended to show small increases in C concentrations while C-poor species showed steep increases in C concentrations. Likewise, the decline in foliar N was largest for species with initially high N concentrations and relatively small for initially low-N species. Despite asymptotic increases in foliar C (Figure 4a), steeper increases in C_i (Figure 3c) translate to average declines in both internal leaf C/C_i ratios of −17 ± 4% with the historical rise in eCO_2, suggesting progressively diminishing returns on C accumulation per unit CO_2 uptake. Similarly, declines in foliar N (Figure 4b) translate to an average N/C_i decline of −30 ± 8%. By applying these functional C_i relationships to projected aCO_2 of 935.8 ppm for year 2100 we estimate that the average foliar C_i would be 641.2 ± 40.6 ppm, foliar C would rise by 10% (from 457 ± 21 mg/g to 505 ± 26 mg/g), N would decline by 12% (from 13.2 ± 0.2 mg/g to 11.6 ± 0.1 mg/g), and C:N ratios would increase by 18% (from 42.9 ± 5.9 to 50.5 ± 2.6) relative to 2016.

4 | DISCUSSION

We document extensive vegetative greening of North America's northern grassland biome over the last two decades. This trend is consistent with widespread and large increases in plant foliar C_i and iWUE that correspond to the rise in eCO_2 since the 1970s. While net vegetative greening rates were most pronounced in the driest and warmest areas of our study region, the direction and magnitude of long-term changes in foliar C_i, iWUE, C, N, and $\delta^{15}N$ did not vary across climates. The spatial uniformity of changes in foliar chemistry across the broad climate gradients sampled contrast with the climate dependency of recent greening and suggests that any realized gains in vegetative growth due to direct effects of eCO_2 at the leaf level were modulated by climate. We find that grassland vegetation across our diverse study area has become increasingly water conservative, C rich, and N poor over the last century.

Across the NGP, NDVI increased on average 0.28% per year, a value similar to model projections for the broader NGP spatial domain over the next century (0.19%–0.45% per year; Hufkens et al., 2016; Reeves et al., 2014). Our finding of higher net greening rates in the NGP than in the NRM is consistent with larger increases in growing season precipitation and decreasing vapor pressure deficit in the NGP than the NRM since the mid-1980s (Bromley et al., 2020; Gerken, Bromley, & Stoy, 2017) but is also likely influenced by the smaller areal distribution of grassland vegetation in the NRM.

Overall, annual net primary production is substantially higher in the NRM compared to the grassland-dominated NGP. However, forest vegetation across much of the NRM has been subject to wildfire and insect-outbreak mortality over the last few decades (Emmett, Renwick, & Poulter, 2019) while the NGP has not, consistent with the lower per-pixel positive greening rate and spatially more extensive vegetative browning rate. While our foliar analyses focused entirely on grassland plant species, our analysis of peak NDVI changes did not distinguish between grassland and forest vegetation. Despite these differences, our finding of increasing iWUE among common plant species distributed across broad climate gradients suggests a direct effect of eCO_2, an inference supported by the timing of sharp increases in iWUE beginning in the 1970s which preceded regional increases in precipitation and water availability (Bromley et al., 2020; Rodell et al., 2018) by decades.

Constant C_i/C_a ratios across modern climates suggests that plants have uniformly adjusted stomatal regulation in response to eCO_2. Our findings of constant and climate-independent increases iWUE with rising CO_2 are consistent with optimal stomatal regulation theory (Farquhar, von Caemmerer, & Berry, 1980), FACE observations (Medlyn et al., 2011), and vegetation paleo-isotope results from other regions (Frank et al., 2015), and provide support for the generality of a strong direct effect of eCO_2 on foliar water–CO_2 exchange. That the NGP has experienced significant increases in vegetative productivity over the last few decades is also consistent with a direct contribution of enhanced photosynthesis to increased iWUE (Guerrieri et al., 2019).

The difference in the timing of historical changes in foliar C_i versus N concentrations offers insight into the degree to which these changes were physiologically coordinated in response to eCO_2 or were independent responses to different forcings. We document a sustained decline in plant N and δ^{15}N that preceded the rise in eCO_2 and recent greening by over a half century. While CO_2 levels during the 1930s were elevated relative to pre-industrial concentrations (~5%), the growth in eCO_2 did not accelerate until the 1960s. Nevertheless, given that N availability in the NGP is low (Burke et al., 1997), it is possible that marginal increases in CO_2 prior to the 1930s increased N demand sufficiently to lower soil N, although such declines in foliar N have been experimentally observed to occur only after doubling of CO_2 (Leakey et al., 2009). Another possibility is that changes in N inputs contributed to the decline in foliar N and δ^{15}N. However, N deposition to our study region is low, and while N deposition has increased by greater than twofold over the last couple of decades (from ~0.6 to ~1.6 kg N ha^{-1} year^{-1}) this represents only ~3%–7% of N mineralization (i.e., internal N supply to plants) across the NGP (Burke et al., 1997). While we do not have measures of the isotopic signature of N deposition across our study area, nor how it has changed over time, attribution of the isotopic shift to atmospheric deposition would imply substantial reliance on this source for plant assimilation and would require an isotopic signature lower than generally recorded (Houlton & Bai, 2009). Moreover, any increase in N supply should yield increases in foliar N, not decreases as we observe.

Our break point analysis suggests an alternative explanation for the onset of N and δ^{15}N declines that may have resulted from a climatic and/or land-use perturbation. The documented declines in N and δ^{15}N in the 1930s show a tight temporal correspondence to an historically unprecedented drought during the Dust Bowl (Fye, Stahle, & Cook, 2003). Though we lack information on potential mechanisms involved (e.g., soil erosion, loss of microbial soil crusts), our finding is broadly consistent with similar herbarium analyses from Central Great Plains grasslands which also document the onset of foliar N and δ^{15}N declines in the 1930s (McLauchlan et al., 2010). Indeed, our study region was among the most strongly affected by the Dust Bowl and was severe in effect across both the NGP and NRM (Fye et al., 2003), consistent with our finding that N declines were independent of ecoregion among common plant species. Regardless of what initially triggered declines in N and δ^{15}N, the fact that they have not recovered to pre-1930's levels, but rather have continued to decline, is consistent with diminished foliar N in the face of sustained eCO_2.

While declines in foliar δ^{15}N are consistent with diminished soil N availability, we lack information on how any increases in biomass production and leaf mass area (LMA; g/m^2) may have influenced declines in foliar N concentrations. FACE experiments document increased LMA in response to eCO_2 (Poorter, Niinemets, Poorter, Wright, & Villar, 2009) and higher declines in N concentrations when expressed per unit leaf mass rather than area (Temme et al., 2017). However, syntheses of FACE results also indicate that declines in foliar N are not explained by dilution from enhanced biomass growth but rather declines in N acquisition and assimilation (Feng et al., 2015), consistent with widespread declines in foliar δ^{15}N in response to eCO_2 (BassiriRad et al., 2003). Nevertheless, we do observe relatively large increases in C concentrations among grasses, which could dilute N assuming constant LMA. A large body of evidence indicates that increases in foliar C under eCO_2 result largely from an increase in non-structural carbohydrates (Leakey et al., 2009; Peñuelas & Estiarte, 1996). Though it remains unclear what specific mechanisms contributed to increased foliar C in our study, we note that grasses can accumulate high levels of silicon (Si) in their leaves, particularly in drier grasslands similar to ours, and tradeoff Si for C as foliar C increases, especially in low-N soils (Quigley, Griffith, Donati, & Anderson, 2020). Furthermore, grass Si concentrations have been shown to decline while phenolic compounds increase in response to eCO_2 (Johnson & Hartley, 2018), suggesting that our documented increases in foliar C may have also been accompanied by changes in Si versus C-based structural support and herbivore defense.

Increasing foliar C and decreasing foliar N suggest that C:N ratios will continue to rise (Figure 4b), a trend that could further constrain plant N supply through greater microbial N immobilization in soils (Feng et al., 2015; Luo et al., 2004). In addition, increases in foliar C:N are associated with decreased leaf protein content and indicate diminished plant nutritional quality for herbivores (Craine, Elmore, & Angerer, 2017; Leakey et al., 2009; Loladze, 2002). Given our evidence for spatially uniform declines in plant N yet climate dependency of greening trends, it is possible that projected increases in precipitation and temperature

(Stoy et al., 2018) will induce further N deficits and poorer quality forage across the NGP.

In addition to the implications of our results for NGP productivity and herbivore responses, our results have direct implications for how Earth system and vegetation models are parameterized. First, our results confirm constant C_i/C_a and increases in iWUE over the last century, a result that is critical to accurate representation of physiological responses to eCO_2. Yet, the implications of increased iWUE for soil water availability and feedbacks to the N cycle (e.g., mineralization and losses) remain highly uncertain. Second, documented declines in foliar N and $\delta^{15}N$ have not been integrated into current land models (Thomas, Brookshire, & Gerber, 2015) but could provide an important constraint to representation of N limitation in simulations of vegetation response to eCO_2 and climate change. Indeed, vegetative greening in the face of declining foliar N and N/C_i suggests a sustained increase in NUE over the last two decades or more, but it is unclear whether such apparent NUE enhancement will persist in the future.

Our results signal a looming threshold in the ability of N to sustain observed greening trends in NGP grasslands, and support the mounting evidence for declines in plant N availability with eCO_2 across N-limited land areas (Craine et al., 2018; McLauchlan et al., 2017). Future plant and subsequent ecosystem responses will depend on the extent that physiological adjustments, allocation patterns, and shifts in N-acquisition strategies (Terrer et al., 2018) may be sufficient to overcome N limitation. Overall, our findings emphasize the importance of understanding historical changes in biogeochemical functioning for next-generation projections of vegetation responses to eCO_2 and climate.

CONFLICT OF INTERESTS

The authors declare no competing financial interests.

AUTHOR CONTRIBUTION

E.N.J.B. designed the study and led data analysis and writing of the paper with help from P.C.S., B.C., and B.F. B.F. performed IRMS analyses.

DATA AVAILABILITY STATEMENT

The data that support the findings of this study are available from the corresponding author upon reasonable request.

ORCID

E. N. Jack Brookshire (iD) https://orcid.org/0000-0002-0412-7696

REFERENCES

Anderson, D. R. (2007). *Model based inference in the life sciences: A primer on evidence*. New York, NY: Springer Science & Business Media.

Auch, R. F., Sayler, K. L., Napton, D. E., Taylor, J. L., & Brooks, M. S. (2011). Ecoregional differences in late-20th-century land-use and land-cover change in the US northern great plains. *Great Plains Research*, *21*, 231–243.

BassiriRad, H., Constable, J. V. H., Lussenhop, J., Kimball, B. A., Norby, R. J., Oechel, W. C., … Silim, S. (2003). Widespread foliage $\delta^{15}N$ depletion under elevated CO_2: Inferences for the nitrogen cycle. *Global Change Biology*, *9*(11), 1582–1590. https://doi.org/10.1046/j.1365-2486.2003.00679.x

Bromley, G. T., Gerken, T., Prein, A. F., & Stoy, P. C. (2020). Recent trends in the near-surface climatology of the northern North American Great Plains. *Journal of Climate*, *33*(2), 461–475. https://doi.org/10.1175/JCLI-D-19-0106.1

Brookshire, E. N. J., & Weaver, T. (2015). Long-term decline in grassland productivity driven by increasing dryness. *Nature Communications*, *6*. https://doi.org/10.1038/ncomms8148

Burke, I. C., Lauenroth, W. K., & Parton, W. J. (1997). Regional and temporal variation in net primary production and nitrogen mineralization in grasslands. *Ecology*, *78*(5), 1330–1340. https://doi.org/10.1890/0012-9658(1997)078[1330:RATVIN]2.0.CO;2

Busch, F. A., Sage, R. F., & Farquhar, G. D. (2018). Plants increase CO_2 uptake by assimilating nitrogen via the photorespiratory pathway. *Nature Plants*, *4*(1), 46–54. https://doi.org/10.1038/s41477-017-0065-x

Craine, J. M., Brookshire, E. N. J., Cramer, M. D., Hasselquist, N. J., Koba, K., Marin-Spiotta, E., & Wang, L. (2015). Ecological interpretations of nitrogen isotope ratios of terrestrial plants and soils. *Plant and Soil*, *396*(1–2), 1–26. https://doi.org/10.1007/s11104-015-2542-1

Craine, J. M., Elmore, A. J., Aidar, M. P. M., Bustamante, M., Dawson, T. E., Hobbie, E. A., … Wright, I. J. (2009). Global patterns of foliar nitrogen isotopes and their relationships with climate, mycorrhizal fungi, foliar nutrient concentrations, and nitrogen availability. *New Phytologist*, *183*(4), 980–992. https://doi.org/10.1111/j.1469-8137.2009.02917.x

Craine, J. M., Elmore, A., & Angerer, J. P. (2017). Long-term declines in dietary nutritional quality for North American cattle. *Environmental Research Letters*, *12*(4), 044019. https://doi.org/10.1088/1748-9326/aa67a4

Craine, J. M., Elmore, A. J., Wang, L., Aranibar, J., Bauters, M., Boeckx, P., … Zmudczyńska-Skarbek, K. (2018). Isotopic evidence for oligotrophication of terrestrial ecosystems. *Nature Ecology & Evolution*, *2*(11), 1735–1744. https://doi.org/10.1038/s41559-018-0694-0

Emmett, K. D., Renwick, K. M., & Poulter, B. (2019). Disentangling climate and disturbance effects on regional vegetation greening trends. *Ecosystems*, *22*(4), 873–891. https://doi.org/10.1007/s10021-018-0309-2

Farquhar, G. D., Ehleringer, J. R., & Hubick, K. T. (1989). Carbon isotope discrimination and photosynthesis. *Annual Review of Plant Physiology and Plant Molecular Biology*, *40*(1), 503–537. https://doi.org/10.1146/annurev.pp.40.060189.002443

Farquhar, G. D., von Caemmerer, S., & Berry, J. A. (1980). A biochemical model of photosynthetic CO_2 assimilation in leaves of C_3 species. *Planta*, *149*(1), 78–90. https://doi.org/10.1007/BF00386231

Feng, Z., Rütting, T., Pleijel, H., Wallin, G., Reich, P. B., Kammann, C. I., … Uddling, J. (2015). Constraints to nitrogen acquisition of terrestrial plants under elevated CO_2. *Global Change Biology*, *21*(8), 3152–3168. https://doi.org/10.1111/gcb.12938

Francey, R. J., Allison, C. E., Etheridge, D. M., Trudinger, C. M., Enting, I. G., Leuenberger, M., … Steele, L. P. (1999). A 1000-year high precision record of $\delta^{13}C$ in atmospheric CO_2. *Tellus B: Chemical and Physical Meteorology*, *51*(2), 170–193. https://doi.org/10.1034/j.1600-0889.1999.t01-1-00005.x

Frank, D. C., Poulter, B., Saurer, M., Esper, J., Huntingford, C., Helle, G., … Weigl, M. (2015). Water-use efficiency and transpiration across

European forests during the Anthropocene. *Nature Climate Change*, 5(6), 579–583. https://doi.org/10.1038/nclimate2614

Fye, F. K., Stahle, D. W., & Cook, E. R. (2003). Paleoclimatic analogs to twentieth-century moisture regimes across the United States. *Bulletin of the American Meteorological Society*, 84(7), 901–910. https://doi.org/10.1175/BAMS-84-7-901

Gerken, T., Bromley, G. T., & Stoy, P. C. (2017). Surface moistening trends in the northern North American Great Plains increase the likelihood of convective initiation. *Journal of Hydrometeorology*, 19(1), 227–244. https://doi.org/10.1175/JHM-D-17-0117.1

Guerrieri, R., Belmecheri, S., Ollinger, S. V., Asbjornsen, H., Jennings, K., Xiao, J., ... Richardson, A. D. (2019). Disentangling the role of photosynthesis and stomatal conductance on rising forest water-use efficiency. *Proceedings of the National Academy of Sciences of the United States of America*, 116(34), 16909–16914. https://doi.org/10.1073/pnas.1905912116

Houlton, B., & Bai, E. (2009). Imprint of denitrifying bacteria on the global terrestrial biosphere. *Proceedings of the National Academy of Sciences of the United States of America*, 106(51), 21713–21716. https://doi.org/10.1073/pnas.0912111106

Huang, K., Xia, J., Wang, Y., Ahlström, A., Chen, J., Cook, R. B., ... Luo, Y. (2018). Enhanced peak growth of global vegetation and its key mechanisms. *Nature Ecology & Evolution*, 2(12), 1897–1905. https://doi.org/10.1038/s41559-018-0714-0

Hufkens, K., Keenan, T. F., Flanagan, L. B., Scott, R. L., Bernacchi, C. J., Joo, E., ... Richardson, A. D. (2016). Productivity of North American grasslands is increased under future climate scenarios despite rising aridity. *Nature Climate Change*, 6(7), 710–714. https://doi.org/10.1038/nclimate2942

Hungate, B., Dukes, J., Shaw, M., Luo, Y., & Field, C. (2003). Nitrogen and climate change. *Science*, 302(5650), 1512–1513.

Johnson, S. N., & Hartley, S. E. (2018). Elevated carbon dioxide and warming impact silicon and phenolic-based defences differently in native and exotic grasses. *Global Change Biology*, 24(9), 3886–3896. https://doi.org/10.1111/gcb.13971

Karger, D. N., Conrad, O., Böhner, J., Kawohl, T., Kreft, H., Soria-Auza, R. W., ... Kessler, M. (2017). Climatologies at high resolution for the earth's land surface areas. *Scientific Data*, 4, 170122. https://doi.org/10.1038/sdata.2017.122

Keeling, C. D., Chin, J. F. S., & Whorf, T. P. (1996). Increased activity of northern vegetation inferred from atmospheric CO_2 measurements. *Nature*, 382(6587), 146–149. https://doi.org/10.1038/382146a0

Lavin, M., & Seibert, C. (2011). Great plains flora? Plant geography of eastern Montana's lower elevation shrub-grass dominated vegetation. *Natural Resources and Environmental Issues*, 16(1), 2.

Leakey, A. D. B., Ainsworth, E. A., Bernacchi, C. J., Rogers, A., Long, S. P., & Ort, D. R. (2009). Elevated CO_2 effects on plant carbon, nitrogen, and water relations: Six important lessons from FACE. *Journal of Experimental Botany*, 60(10), 2859–2876. https://doi.org/10.1093/jxb/erp096

Loladze, I. (2002). Rising atmospheric CO_2 and human nutrition: Toward globally imbalanced plant stoichiometry? *Trends in Ecology & Evolution*, 17(10), 457–461. https://doi.org/10.1016/S0169-5347(02)02587-9

Luo, Y., Su, B., Currie, W., Dukes, J., Finzi, A., Hartwig, U., ... Field, C. (2004). Progressive nitrogen limitation of ecosystem responses to rising atmospheric carbon dioxide. *BioScience*, 54(8), 731–739. https://doi.org/10.1641/0006-3568(2004)054[0731:PNLOER]2.0.CO;2

Mao, J., Ribes, A., Yan, B., Shi, X., Thornton, P. E., Séférian, R., ... Lian, X. U. (2016). Human-induced greening of the northern extratropical land surface. *Nature Climate Change*, 6(10), 959–963. https://doi.org/10.1038/nclimate3056

McLauchlan, K. K., Ferguson, C. J., Wilson, I. E., Ocheltree, T. W., & Craine, J. M. (2010). Thirteen decades of foliar isotopes indicate declining nitrogen availability in central North American grasslands. *New Phytologist*, 187(4), 1135–1145. https://doi.org/10.1111/j.1469-8137.2010.03322.x

McLauchlan, K. K., Gerhart, L. M., Battles, J. J., Craine, J. M., Elmore, A. J., Higuera, P. E., ... Perakis, S. S. (2017). Centennial-scale reductions in nitrogen availability in temperate forests of the United States. *Scientific Reports*, 7(1), 7856. https://doi.org/10.1038/s41598-017-08170-z

McMurtrie, R. E., Norby, R. J., Medlyn, B. E., Dewar, R. C., Pepper, D. A., Reich, P. B., & Barton, C. V. (2008). Why is plant-growth response to elevated CO_2 amplified when water is limiting, but reduced when nitrogen is limiting? A growth-optimisation hypothesis. *Functional Plant Biology*, 35(6), 521–534. https://doi.org/10.1071/FP08128

Medlyn, B. E., Duursma, R. A., Eamus, D., Ellsworth, D. S., Prentice, I. C., Barton, C. V., ... Wingate, L. (2011). Reconciling the optimal and empirical approaches to modelling stomatal conductance. *Global Change Biology*, 17(6), 2134–2144. https://doi.org/10.1111/j.1365-2486.2010.02375.x

Mueggler, W. F., Stewart, W. L., US Forest Service, & Intermountain Forest and Range Experiment Station. (1980). Grassland and shrubland habitat types of western Montana. In *US Forest Service, Intermountain Forest and Range Experiment Station, General Technical Report, INT-66*. Retrieved from http://www.cabdirect.org/abstracts/19802604329.html

Myneni, R. B., Keeling, C. D., Tucker, C. J., Asrar, G., & Nemani, R. R. (1997). Increased plant growth in the northern high latitudes from 1981 to 1991. *Nature*, 386(6626), 698–702. https://doi.org/10.1038/386698a0

Peñuelas, J., & Estiarte, M. (1996). Trends in plant carbon concentration and plant demand for N throughout this century. *Oecologia*, 109(1), 69–73. https://doi.org/10.1007/s004420050059

Peñuelas, J., & Matamala, R. (1990). Changes in N and S leaf content, stomatal density and specific leaf area of 14 plant species during the last three centuries of CO_2 increase. *Journal of Experimental Botany*, 41(9), 1119–1124. https://doi.org/10.1093/jxb/41.9.1119

Poorter, H., Niinemets, Ü., Poorter, L., Wright, I. J., & Villar, R. (2009). Causes and consequences of variation in leaf mass per area (LMA): A meta-analysis. *New Phytologist*, 182(3), 565–588. https://doi.org/10.1111/j.1469-8137.2009.02830.x

Quigley, K. M., Griffith, D. M., Donati, G. L., & Anderson, T. M. (2020). Soil nutrients and precipitation are major drivers of global patterns of grass leaf silicification. *Ecology*, e03006. https://doi.org/10.1002/ecy.3006

Reeves, M. C., Moreno, A. L., Bagne, K. E., & Running, S. W. (2014). Estimating climate change effects on net primary production of rangelands in the United States. *Climatic Change*, 126(3–4), 429–442. https://doi.org/10.1007/s10584-014-1235-8

Reich, P. B., & Hobbie, S. E. (2013). Decade-long soil nitrogen constraint on the CO_2 fertilization of plant biomass. *Nature Climate Change*, 3(3), 278–282. https://doi.org/10.1038/nclimate1694

Rodell, M., Famiglietti, J. S., Wiese, D. N., Reager, J. T., Beaudoing, H. K., Landerer, F. W., & Lo, M.-H. (2018). Emerging trends in global freshwater availability. *Nature*, 557(7707), 651–659. https://doi.org/10.1038/s41586-018-0123-1

Shafer, S. L., Bartlein, P. J., Gray, E. M., & Pelletier, R. T. (2015). Projected future vegetation changes for the northwest United States and southwest Canada at a fine spatial resolution using a dynamic global vegetation model. *PLoS ONE*, 10(10), e0138759. https://doi.org/10.1371/journal.pone.0138759

Still, C. J., Berry, J. A., Collatz, G. J., & DeFries, R. S. (2003). Global distribution of C_3 and C_4 vegetation: Carbon cycle implications. *Global Biogeochemical Cycles*, 17(1), 6-1–6-14. https://doi.org/10.1029/2001GB001807

Stoy, P. C., Ahmed, S., Jarchow, M., Rashford, B., Swanson, D., Albeke, S., … Poulter, B. (2018). Opportunities and trade-offs among BECCS and the food, water, energy, biodiversity, and social systems nexus at regional scales. *BioScience*, *68*(2), 100–111. https://doi.org/10.1093/biosci/bix145

Temme, A. A., Liu, J. C., van Hal, J., Cornwell, W. K., Cornelissen, J. H. H., & Aerts, R. (2017). Increases in CO_2 from past low to future high levels result in "slower" strategies on the leaf economic spectrum. *Perspectives in Plant Ecology, Evolution and Systematics*, *29*, 41–50. https://doi.org/10.1016/j.ppees.2017.11.003

Terrer, C., Vicca, S., Stocker, B. D., Hungate, B. A., Phillips, R. P., Reich, P. B., … Prentice, I. C. (2018). Ecosystem responses to elevated CO_2 governed by plant–soil interactions and the cost of nitrogen acquisition. *New Phytologist*, *217*(2), 507–522. https://doi.org/10.1111/nph.14872

Thomas, R. Q., Brookshire, E. N. J., & Gerber, S. (2015). Nitrogen limitation on land: How can it occur in Earth system models? *Global Change Biology*, *21*(5), 1777–1793. https://doi.org/10.1111/gcb.12813

Zhu, Z., Piao, S., Myneni, R. B., Huang, M., Zeng, Z., Canadell, J. G., … Zeng, N. (2016). Greening of the Earth and its drivers. *Nature Climate Change*, *6*(8), 791–795. https://doi.org/10.1038/nclimate3004

SUPPORTING INFORMATION

Additional supporting information may be found online in the Supporting Information section.

How to cite this article: Brookshire ENJ, Stoy PC, Currey B, Finney B. The greening of the Northern Great Plains and its biogeochemical precursors. *Glob Change Biol*. 2020;00:1–10. https://doi.org/10.1111/gcb.15115